The Journal of the Korean Society of Oceanography
Vol. 29, No. 3, pp. 248-257, September 1994

Uranium-Series Growth Rates of Two Manganese Nodules from the KODOS-89 Site, Clarion-Clipperton Fracture Zones of the Central Equatorial Pacific

DEOK SOO MOON*, KEE HYUN KIM* AND JUNG KEUK KANG**
*Dept. of Oceanography, Chungnam National University, Taejon 305-764, Korea
**Korea Ocean Research and Development Institute, Ansan 425-600, Korea

우라늄 계열 기법으로 측정된 클라리온-클리퍼톤 균열대 KODOS-89 지역 망간단괴 2개의 성장속도

문덕수* · 김기현* · 강정극**
*충남대학교 해양학과, 대전 305-764
**한국해양연구소, 안산 425-600

Growth rates of two manganese nodules collected in the Korea Deep Ocean Study (KODOS-89) site in the Clarion-Clipperton Fracture Zones in the central Equatorial Pacific have been estimated by employing uranium-series disequilibrium techniques to investigate the geochemical processes leading to the formation of deep-sea nodules. The growth rates estimated from the profiles of excess ^{230}Th activities and ratios of excess ^{230}Th to ^{232}Th are in the order of a few millimeters per million years. Growth rates at bottom-side of nodules are 2-3 times faster than those at top-sides. Diagenetic supply of manganese could explain the faster growth at the bottom-side of nodules.

심해저 망간단괴가 성장할 때 단괴 주변에서 작용하는 지화학적 과정들을 구명 하기 위하여 클라리온-클리퍼톤 균열대의 한국심해연구 (KODOS-89) 지역에서 채취한 망간 단괴에 대하여 우라늄계열 비평형기법을 적용하여 성장속도가 추정되고 그 지화학적 의미가 해석되었다. 과잉 230-Th 방사능과 이 값의 232-Th에 대한 방사능비의 수직적 분포로부터 추정된 두 망간단괴의 성장 속도는 백만년 당 수 밀리미터 정도였다. 퇴적물과 접해 있는 단괴 아래쪽 부분의 성장속도는 해수와 접해있는 윗쪽 부분의 성장속도보다 2~3배 빠르다. 단괴의 바닥부분이 빠르게 성장하는 것은 속성작용에 의한 망간의 공급으로 인한 것으로 사료된다.

INTRODUCTION

Ferromanganese nodules are authigenic formation of iron and manganese oxides on the deep-sea floor. The high contents of various strategic metals such as cobalt, nickel and copper in Mn nodules make them be considered as potential resources. Many studies of manganese nodules have been directed toward resolving puzzles regarding their origin, growth history, and metal geochemistry. A multi-institutional research program, Manganese Nodule Program (MANOP), has studied the genesis of manganese nodules and abyssal geochemistry at MANOP sites H (hemipelagic), S (siliceous ooze), and R (red clay) in the north Pacific (Moore *et al.*, 1981; Bender, 1983; Dymond *et al.*, 1984; Finney *et al.*, 1984; Huh and Ku, 1984; Moore, 1984). The biological productivity and particulate flux to the seafloor decrease in order of site H, S, and R (Bender, 1983). The growth pro-

cess of nodules at sites S and R is both hydrogenous and oxic diagenesis (Dymond *et al.*, 1984).

Major components of nodules are manganese dioxide (MnO_2) and iron oxide (Fe_2O_3). Major minerals of nodules are vernadite, todorokite and birnessite. Nodules are classified into 3 groups, hydrogenous, diagenetic, and hydrothermal in origin, on the basis of element sources indicated by the major minerals. Hydrogenous nodules of vernadite form by direct precipitation or accumulation of colloidal metal oxides from seawater, whereas diagenetic nodules of todorokite accrete Mn liberated by diagenetic alteration of sediments and grow down into the sediment column (Calvert and Price, 1977). Remineralization of metals in sediment and the subsequent upward diffusion through pore water are most probable processes leading to the diagenetic formation of nodules. Hydrothermal nodules of birnessite form near the spreading centers and submarine volcanoes (Moorby *et al.*, 1984).

Uranium-series disequilibrium techniques have been applied to determine growth rates of Mn nodules. Earlier estimation of nodule growth rates in the order of 1~100 mm/ky from the inward decreases of ^{226}Ra (Pettersson, 1955; Von Buttlar and Houterman, 1950) turned out to be an overestimation caused by the existence of supported ^{226}Ra by its parent ^{230}Th within the nodules (Goldberg and Arrhenius, 1958). Based on the distributions of $^{230}Th_{xs}$ and $^{230}Th_{xs}/^{232}Th$ (where $^{230}Th_{xs}$ = Excess $^{230}Th = ^{230}Th_{total} - ^{234}U$), the growth rates of Mn nodules were revised to be in the order of 1~100 mm/My (Ku and Broecker, 1969; Ku, 1977; Ku *et al.*, 1977; Andersen and MacDougall, 1977; Krishnaswami and Cochran, 1978; Ku and Knauss, 1979; Moore *et al.*, 1981; Huh and Ku, 1984). The slow rates of 1~100 mm/My have been supported by other radiometric and non-radiometric growth rates deduced from ^{10}Be and ^{26}Al profiles (Guichard *et al.*, 1978; Turekian *et al.*, 1979; Sharma and Somayajulu, 1982; Krishnaswami *et al.*, 1978; Segl *et al.*, 1989); hydration rind dating (Burnett and Morgenstein, 1976); biostratigraphy (Harada and Nishida, 1976; Kadko and Burckle, 1980); amino acid dating using the racemization of isoleucine (Bada, 1972); stratigraphic interpretation (Von Stackelberg, 1979); comparison of burial rates, growth rates and size distribution of nodules (Heath, 1979); K/Ar dating of basalt nuclei (Barnes and Dymond, 1967); paleomagnetic stratigraphy (Crecelius *et al.*, 1973).

Most of deep-sea nodules are found lying on the surface of sediment. While these nodules accrete at rates of 1~10 mm/My, the sediment underlying the nodules accumulates at rates of about 1~10 mm/ky. It is questioned why nodules are not buried by the avalanche of sediment. In an effort to answer the question, diverse hypotheses have been suggested, including bioturbation (Piper and Fowler, 1980) and ocean bottom current (Glasby, 1973) which rolls the nodules around. The turnover time of nodules is estimated to be 1~100 ky using ^{230}Th difference between the top and bottom sides of nodules (Krishnaswami and Cochran, 1978; Huh and Ku, 1984).

A number of manganese nodules and sediment cores were collected in Korea Deep Ocean Study (KODOS) site in the CCFZ during 1989~1992 (KORDI, 1990; 1992). Sedimentation rates in KODOS area were estimated to be 0.2 mm/ky by biostratigraphy (KORDI, 1991) and 0.29~1.61 mm/ky by excess ^{230}Th techniques (Moon, 1993). Hydrogenous nodules occur on abyssal hills in this area, whereas diagenetic nodules are distributed on abyssal plain (Kang and Han, 1988; Jung *et al.*, 1990).

The purpose of this study is thus twofold: 1) to estimate the growth rates of manganese nodules by employing uranium-series disequilibrium techniques, and 2) to investigate the geochemical processes acting in manganese nodules and their associated sediments. Results from this study will shed some light on the origin and formation processes of the Pacific manganese nodules in the KODOS-89 site.

MATERIALS AND METHODS

On-board works

Nodule samples analyzed in this study were collected from the KODOS-89 sites located between

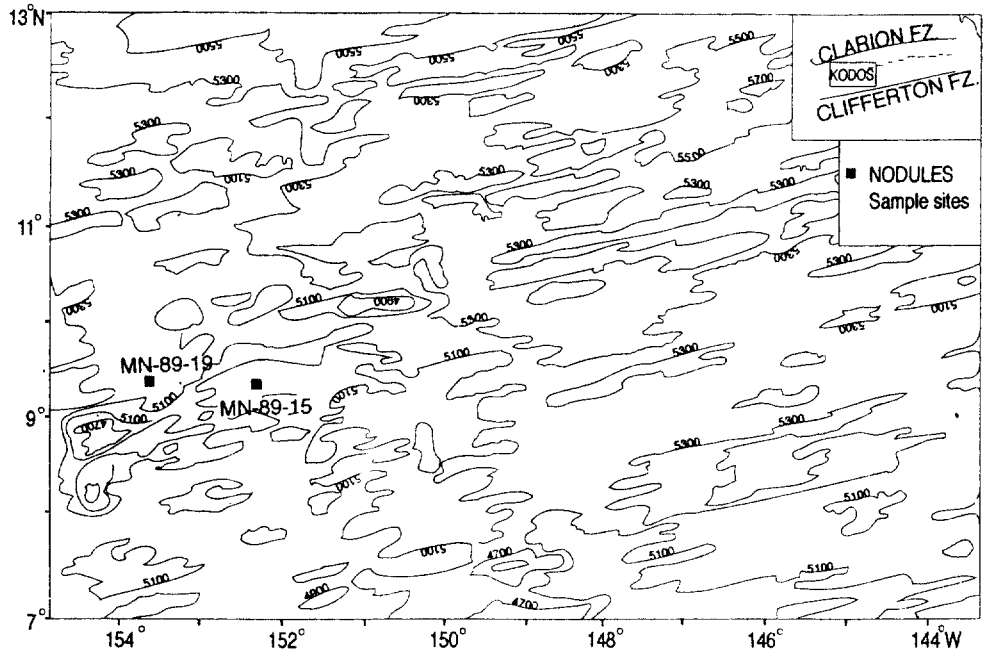

Fig. 1. Bathymetry map of KODOS area showing the location of sampling area. Water depth in meters.

Table 1. Location, water depth (m) and sea-bottom feature of coring sites, and average size of their associated nodules

Station	Nodule I.D.	Location		Water	Bottom	Dimension of nodule
		Latitude (N)	Longitude (E)	Depth (m)	Topography	(L*W*H) (mm)
KODOS89-15	MN-89-15	9° 20′	152° 40′	5,212	Abyssal plain	35×20×15
KODOS89-19	MN-89-19	9° 40′	153° 22′	4,800	Seamount	47×43×30

the Clarion and Clipperton fracture zones (CCFZ), east of the Line Islands Ridge in central Equatorial Pacific (Fig. 1) during *R/V Farnella* cruise in 1989 by KORDI. The location and water depth of sampling sites is presented in Table 1 and Fig. 1 (KORDI, 1990; 1991).

Undisturbed manganese nodules and surface sediments were sampled using a box corer. Immediately after the corer was retrieved onto the deck, seawater overlying the sediment was carefully siphoned off to photograph the nodules on sediment surface. Nodules were hand-picked, washed with seawater, sealed in vinyl bags, and preserved in refrigerator until analyzed. After the removal of nodules, subcores of sediment were carefully taken by inserting clear acrylic pipes (diameter 8 cm) into the sediment by hand.

Sample preparation

Contiguous veneers of relatively uniform thickness of nodule material were scraped off from nodule surface with a known area using a dental drill. The thickness of each sampling interval was calculated by:

$$\text{thickness (cm)} = \frac{\text{weight scraped (g)}}{\text{bulk density of nodule (g/cm}^3\text{)} \times \text{area scraped (cm}^2\text{)}}$$

assuming a bulk density of nodule to be 2.0 g/cm^3 (Ku, 1976). The scraped nodule material was dried at 60℃ and sealed in plastic vials and stored in

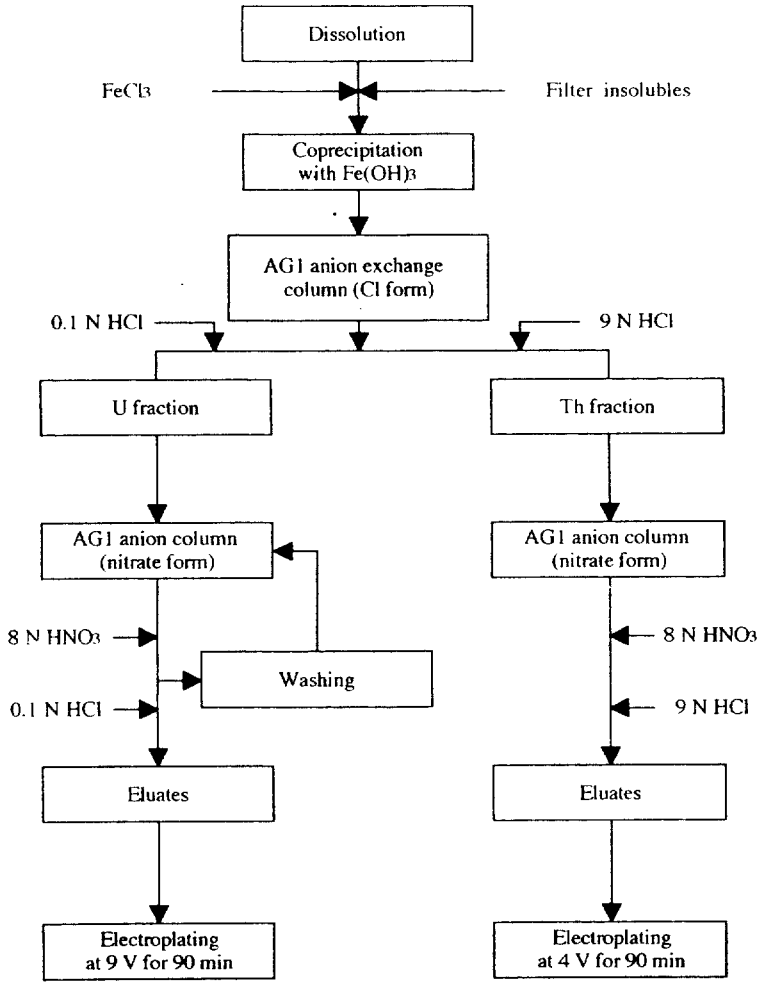

Fig. 2. Flow diagram showing the separation scheme of uranium and thorium isotopes in sediment and nodule samples. Modified after Anderson and Fleer (1982).

a desiccator until analyzed.

Radiochemical Analysis

Fig. 2 shows the outline of separation and purification scheme of U and Th nuclides employed in this study. Details of the analytical procedures could be found elsewhere in literature (Anderson and Fleer, 1982; Huh, 1982). About 20~100 mg of powdered nodule material was leached for one hour in 9N HCl in the presence of ^{232}U and ^{228}Th yield tracer (11.66 dpm/ml). Activities of uranium and thorium isotopes were determined in the acid extracts. Uranium was separated from thorium by anion exchange using Dowex AG1-X8 resin (100~200 mesh, chloride form). For further purification of uranium and thorium, two types of resins were used: a column of untreated AG1 resin (Cl^- form), and the second column of nitrate-type resin converted from the Cl^- form AG1 (Joshi, 1985). The purified U was electroplated at 9 volts, and Th at 4 volts, for 60~90 minutes onto stainless-steel planchets.

Counting

Activities of uranium and thorium isotopes were counted by alpha spectrometry with silicon sur-

face-barrier detectors mounted inside vacuum counting chambers. Detectors with an active surface area of 450 mm^2 and a minimum depletion thickness of 100 μm were connected to a Canberra Series 40 multichannel analyzer with 2K channels per detector, running on PHA mode.

RESULTS AND DISCUSSION

Reported growth rates of deep-sea Mn nodules are in the range of 1~6 mm/My (Huh and Ku, 1984 and references therein). These slow growth rates require a decrease in ^{230}Th activity with factor of two within one tenth of a millimeter, a thickness that cannot be resolved by the available sampling techniques. To overcome this problem, a mean density of the nodules is used to evaluate the thickness of the sampled layer (Ku, 1976). This method of sampling contiguous layers could contaminate inner layers with surface material, yielding an apparent decrease in activity at the surface due to dilution. The possibility of sampling artifact was, however, ruled out by non-destructive alpha track profiles of polished sections of Mn nodules, displaying exponential decreases of alpha emitting nuclides with depth (Heye and Marchig, 1977).

In our estimation of growth rates for the top-side and bottom-side of each nodule, we have employed two different approaches: i) growth rate based on decay profile of the excess ^{230}Th activities ($^{230}Th_{xs}$); and ii) growth rate based on the activity ratios (A.R.) of $^{230}Th_{xs}/^{232}Th$. Two growth rates by the above different approaches were calculated to examine their agreement.

Nodule MN-89-15

The growth rate of the top-side of nodule MN-89-15 was estimated to be 1.17± 0.27 mm/My by $^{230}Th_{xs}$ and 1.22± 0.21 mm/My by A.R. of $^{230}Th_{xs}/^{232}Th$, where errors based on "1-σ standard error" due to regression (Fig. 3, Table 2). The growth rates estimated by the two different approaches agree within their 1-σ standard error (Table 4). Our results are comparable to those reported in previous studies on deep-sea nodules (Krishnaswami and Cochran, 1978; Krishnaswami *et al.*, 1978; Huh and Ku, 1984).

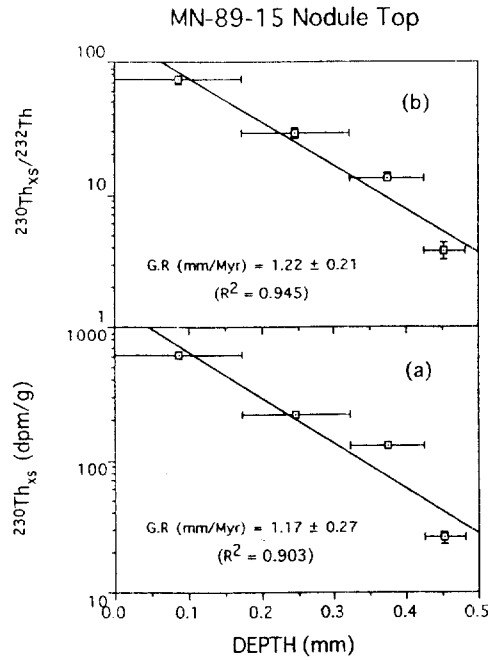

Fig. 3. $^{230}Th_{xs}$ activity (a), and $^{230}Th_{xs}/^{232}Th$ activity ratio (b), as a function of depth in the top side of the nodule MN-89-15. Horizontal bars represent the thickness of sampled layers and the vertical bars 1σ counting statistics. G.R. represents growth rates. Two growth rates derived from both methods are in good agreement.

The growth rates of the bottom-side of the nodule are approximately two times faster than those of the top-side, estimated to be 2.88± 0.62 mm/My by $^{230}Th_{xs}$ and 2.06± 0.29 mm/My by A.R. (Fig. 4). These two estimates of growth rates for the bottom-side of the nodule MN-89-15 by two different techniques agree within their 1-σ standard errors, as in the case of the top-side.

Nodule MN-89-19

The growth rate of the top-side of nodule MN-89-19 was estimated to be 1.41± 0.22 mm/My by $^{230}Th_{xs}$ and 1.18± 0.05 mm/My by A.R. (Fig. 5, Table 3). The two estimates are in agreement within their 1-σ standard errors. The bottom-side of the nodule grew at a rate of 2.90± 0.37 mm/My esti-

Table 2. Results of radiochemical analysis of U and Th nuclides in manganese nodule MN-89-15 (9° 20'N, 152° 40'E· water depth 5,212 m). Ratios are activity ratios and errors quoted are 1σ errors based on counting statistics.

Depth (mm)	U-238 (ppm)	Th-232 (ppm)	Th-230 (dpm/g)	Th-230$_{xs}$ (dpm/g)	Th-230$_{xs}$/Th-232 Activity Ratio
Top-side					
0-0.173	5.89± 1.10	34.6± 2.95	630± 13.5	624± 13.5	73.2± 6.43
0.173-0.322	5.91± 0.85	31.4± 2.71	228± 5.25	223± 5.29	28.8± 2.58
0.322-0.425	12.54± 1.96	38.9± 2.75	140± 3.11	129± 3.43	13.5± 1.02
0.425-0.481	12.04± 2.09	27.5± 2.89	39.1± 1.74	25.8± 2.59	3.81± 0.55
Bottom-side					
0-0.075	4.40± 0.69	20.3± 2.25	363± 7.76	357± 7.79	71.3± 8.05
0.075-0.205	6.68± 0.93	33.0± 2.33	381± 8.04	373± 8.09	45.9± 3.39
0.205-0.285	9.34± 1.12	36.4± 2.76	272± 5.75	265± 5.81	29.6± 2.34
0.285-0.373	8.04± 0.89	36.8± 2.88	129± 3.47	121± 3.55	13.4± 1.12
0.373-0.427	10.55± 2.04	39.0± 4.27	119± 4.31	111± 4.59	11.6± 1.36
0.427-0.546	11.66± 1.38	39.9± 3.62	127± 4.42	117± 4.54	12.0± 1.18

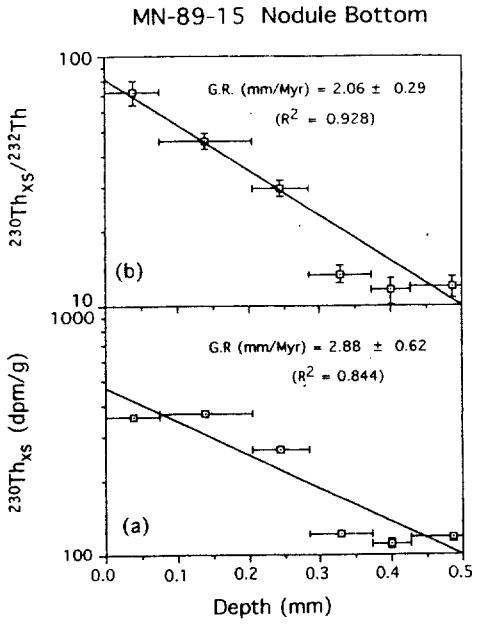

Fig. 4. Profiles of $^{230}Th_{xs}$ activity (a), and $^{230}Th_{xs}/^{232}Th$ activity ratio (b), in bottom side of nodule MN-89-15.

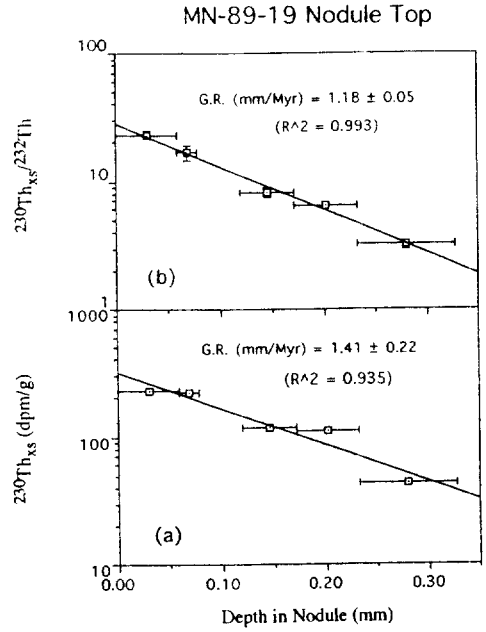

Fig. 5. $^{230}Th_{xs}$ activity (a), and $^{230}Th_{xs}/^{232}Th$ activity ratio (b), as a function of depth in the top side of the nodule MN-89-19. G.R. represents growth rates.

mated by $^{230}Th_{xs}$ and 3.72± 0.26 mm/My by A.R. (Fig. 6). Considering the range of their statistical errors, the two growth rates of the bottom-side show poor agreement. Nevertheless, it seems obvious that the bottom-side of the nodule MN-89-19 grew approximately 2 to 3 times faster than the top-side (Table 4).

Top versus Bottom

Faster growth rates at bottom sides of Mn nodules than at top-sides can be attributed to the supply of the diagenetic manganese to the bottom surface of nodules. The formation of ferromanga-

Table 3. Results of radiochemical analysis of U and Th nuclides in manganese nodule MN-89-19 (9° 40'N, 153° 22'E; water depth 4,800 m). Ratios are activity ratios and errors quoted are 1σ errors based on counting statistics.

Depth (mm)	U-238 (ppm)	Th-232 (ppm)	Th-230 (dpm/g)	Th-230_{xs} (dpm/g)	Th-230_{xs}/Th-232 Activity Ratio
Top-side					
0-0.060	4.31± 0.59	40.3± 2.84	233± 5.29	229± 5.32	23.1± 1.71
0.060-0.078	10.4± 2.03	54.4± 6.85	237± 8.44	224± 8.66	16.8± 2.21
0.078-0.120	N.D.	N.D.	N.D.	N.D.	N.D.
0.120-0.171	8.02± 0.94	57.5± 4.87	124± 4.50	117± 4.56	8.30± 0.77
0.171-0.231	8.75± 0.81	69.4± 3.07	116± 2.53	110± 2.60	6.41± 0.32
0.231-0.327	12.4± 1.25	55.2± 3.27	51.0± 1.84	43.4± 2.02	3.19± 0.24
Bottom-side					
0-0.084	8.82± 0.70	53.7± 2.73	892± 16.2	882± 16.2	66.8± 3.61
0.084-0.167	8.98± 0.98	54.9± 3.31	791± 17.2	775± 17.3	57.5± 3.69
0.167-0.261	8.09± 0.68	53.5± 3.97	591± 16.9	574± 16.9	43.6± 3.48
0.261-0.309	8.48± 0.88	49.5± 3.11	488± 8.79	481± 8.82	39.6± 2.59
0.309-0.396	10.3± 0.45	42.5± 2.46	327± 6.60	319± 6.68	30.5± 1.88

*N.D.: Not Determind

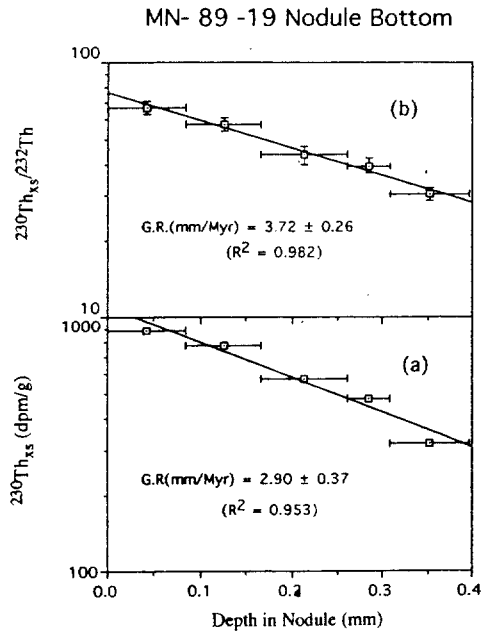

Fig. 6. Profiles of $^{230}Th_{xs}$ activity (a), and $^{230}Th_{xs}/^{232}Th$ activity ratio (b), in bottom side of MN-89-19 nodule.

nese oxides are related to the oxidation of iron and manganese. In deep-sea sediments, Eh value decreases with depth due to the consumption of oxidants. Because Fe^{+2} oxidizes more readily than Mn^{+2}, the depth which marks the Fe^{+3}~Fe^{+2} boundary (commonly indicated by a brown to gray-

Table 4. Growth rates of nodules estimated from the distribution of activities of $^{230}Th_{xs}$ and $^{230}Th_{xs}/^{232}Th$ activity ratios

Nodule ID	Top/ Bottom	Growth Rate(mm/My) Th-230xs	Th-230xs/Th-232
MN-89-15	Top	1.17± 0.21	1.22± 0.21
	Bottom	2.88± 0.62	2.06± 0.29
MN-89-19	Top	1.41± 0.22	1.18± 0.05
	Bottom	2.90± 0.37	3.72± 0.26

green color change) is below the Mn^{+4}~Mn^{+2} boundary. Most of deep-sea sediments in the study area are oxidized enough to have brown clay near the sediment-water interface (Jung *et al.* 1991). The manganese reducing zone (i.e. below the Mn^{+4}~Mn^{+2} boundary), however, may exist at a shallow depth causing Mn^{+2} to diffuse upward in pore water to allow oxidation and incorporation into the nodules (Lynn and Bonatti, 1965). Dymond *et al.* (1984) have divided the nodules of diagenetic origin into two sub-groups: oxic diagenetic and suboxic diagenetic varieties. Oxic diagenesis involves reactions in oxidized sediments that add transition metals to nodules (Heath and Dymond, 1977; Lyle *et al.*, 1984). Suboxic diagenesis is driven by organic carbon utilization of oxidants within the sediment, which results in the reduction of solid phase (Mn^{+4} and Fe^{+3}) to soluble (Mn^{+2} and Fe^{+2}) and subsequent upward diffusion in

pore water (Froelich *et al.*, 1979). This diagenetic component of manganese (Lynn and Bonatti, 19 65) is distinguished from the hydrogenous component of Mn which precipitates directly from sea water (Calvert and Price, 1977). The diagenetic supply of manganese to the bottom-side of nodules on sediments surface would make the growth rates of bottom-side faster than those of top-side.

The faster growth at the bottom sides of the nodules, Mn-89-15 and Mn-89-19, strongly indicates that the major source of metals in the nodules is the remobilization of manganese and other miner metals during diagenetic alteration of sediments and the subsequent upward diffusion of these metals through sediment pore water. Diagenetic processes probably play the major role in the growth at the bottom-sides of nodules in the study area, whereas hydrogenous source plays important role in the growth at the top-sides of the nodules.

Normalization of ^{230}Th Activity

The two thorium isotopes in Mn nodules, ^{230}Th and ^{232}Th, have significantly different geochemical pathways. ^{232}Th in crustal rocks is released by weathering processes, bounded by detrital phases, carried to the ocean, and removed onto the seafloor, whereas ^{230}Th is continuously produced within the water column by the decay of ^{234}U dissolved in seawater and scavenged almost quantitatively by settling particulates down to the seafloor. In order to use ^{232}Th in normalizing ^{230}Th activities, we assumed that no isotopic fractionation occurred and chemical behaviors of the two isotopes are identical throughout the processes of diagenetic alteration of sediments and nodule accretion. Such assumptions are reasonable for the isotopes of the same element with a negligible mass difference of 2/230. Thus their identical chemistry permits the normalization of excess ^{230}Th activity by ^{232}Th.

Our results from two nodules display higher goodness-of-fit values (R^2) of the regression for the plot of normalized $^{230}Th_{xs}/^{232}Th$ ratios than those of $^{230}Th_{xs}$ activity profiles (Fig. 1-Fig. 4). This may demonstrate that the use of the ^{232}Th-normalized ratios are preferable to the use of ^{230}Th activity alone in estimating nodule growth rates.

CONCLUSIONS

Growth rates of two manganese nodules collected from the KODOS-89 site in the CCFZ of the Central Equatorial Pacific are estimated to be in the order of a few millimeters per 10^6 years by applying ^{230}Th as a geochronometer. Growth rates at bottom sides of the nodules are 2~3 times faster than those at top-sides in both cases, indicating different sources of metals between top- and bottom-sides. Diagenetic supply of manganese and other minor metals from the sediment pore water could explain the faster growth rates at the bottom-side of nodules, whereas top-side accretes metals of hydrogenous source.

Although the two thorium isotopes in Mn nodules, ^{230}Th and ^{232}Th, have significantly different geochemical pathways, their similar chemistry during sediment diagenesis allow us the normalization of excess ^{230}Th activity by ^{232}Th. Our results indicate that the use of the normalized ratios are preferable to the use of ^{230}Th activity alone in estimating nodule growth rates.

ACKNOWLEDGMENTS

Manganese nodule samples used in this study were collected during R/V Farnella cruise in the 1989 by the Korea Ocean Research and Development Institute. We are thankful to Hae Kyung Park and Hyun Bum Shin of the Marine Radiochemistry Lab, Chungnam University, for their assistance in laboratory works.

REFERENCES

Andersen, M. E. and J. D. MacDougall, 1977. Accumulation rates of manganese nodules and sediments: an alpha track method. *Geophys. Res. Lett.*, **4**: 351-353.

Anderson, R. F. and A. P. Fleer, 1982. Determination of natural actinides and plutonium in marine particulate material. *Anal. Chem.*, **54**: 1142-1147.

Bada, J. L., 1972. The dating of fossil bones using the racemization of isoleucine. *Earth Planet. Sci. Lett.*,

15: 223-231.

Barnes, S.S. and J. Dymond, 1967, Rates of accumulation of ferromanganese nodules, *Nature*, **213**: 1218-1219.

Bender, M.L., 1983, The Manganese Nodule Project, EOS 64, No. 5: 43-44.

Burnett, W.C. and M. Morgenstein, 1976, Growth rates of Pacific Nodules as deduced by uranium series and hydration rind dating techniques. *Earth Planet. Sci. Lett.*, **33**: 208 - 218.

Calvert, S.E. and N.B. Price, 1977, Geochemical variation in ferromanganese nodules and associated sediments from the Pacific Ocean, *Mar. Chem.*, **5**: 43-74.

Crecelius, E.A., R. Carpenter and R. TR. Merrill ., 1973, Magnetism and magnetic reversalsin ferromanganese nodules, Earth Planet. *Sci. Lett.*, **17**: 391-396.

Dymond, J., M. Lyle, B. Finney, D.Z. Piper, K. Murphy, R. Conard and N. Pisias, 1984, Ferromanganese nodules from MANOP Sites H, S, and R-Control of mineralogical and chemical composition by multiple accretionary processes, *Geochim. Cosmochim. Acta.* **48**: 931-949.

Finney, B., G.R. Health and M. Lyle, 1984, Growth rates of manganese-rich nodules at MANOP Site H, Geochim. Cosmochim. *Acta.* **48**: 911-917.

Froelich, P.N., G.P. Klinkhammer, M.L. Bender, N.A. Luedtke, G.R. Heath, D. Cullen , P. Dauphin, D. Hammond, B. Hartman and V. Maynard, 1979, Early oxidation of organic matter in pelagic sediments of the eastern equatorial Atlantic: suboxic diagenesis, Geochim. Cosmochim. *Acta.* **43**: 1075-1090 .

Glasby, G.P., 1973, Mechanisms of enrichments of the rare earth elements in marine manganese nodules, *Mar. Chem.*, **1**: 105-125.

Goldberg, E.D. and G. Arrhenius, 1958, Chemistry of Pacific pelagic sediments, Geochim. Cosmochim. *Acta.* **13**: 153-212.

Guichard, F., J.-L. Reyss and Y. Yokoyama, 1978, Growth rate of manganese nodule measured with Be-10 and Al-26, *Nature*, **272**: 155-156.

Harada, K. and S. Nishida, 1976, Biostratigraphy of some marine manganese nodules, *Nature*, **260**: 770-771.

Heye, D. and V. Marchig, 1977, Relationship between the growth rate of manganese nodules from the central Pacific and their chemical composition. *Mar. Geol.*, **23**: M19-M25.

Heath, G.R., 1979, Burial rates, growth rates and size distribution of deep-sea manganese nodules, Science, **205**: 903-904.

Heath, G.R. and J. Dymond, 1977, Genesis and transformation of metalliferous sediments from the East Pacific Rise, Bauer Deep and Central Basin, northwest Nazca plate, *Geol. Soc. Am. Bull.*, **80**: 723-733.

Huh, C.A., 1982, Radiochemical and chemical studies of manganese nodules from three sedimentary regimes in the North Pacific. Ph.D. Thesis, University of Southern California, Los Angeles, 305pp.

Huh, C.A. and T.L. Ku, 1984, Radiochemical observations on manganese nodules from three sedimentary environments in the north Pacific, *Geochim. Cosmochim. Acta.*, **48**: 951-963.

Joshi, S.R, 1985, Determination of thorium-228, 230, 232, in sediments by anion exchange and nuclear spectrometer, *Anal. Chem.*, **57**: 1023-1026.

Jung, H.S, J.K. Kang, K.S. Jeong and D.H. Shin, 1991, Geochemical characteristics of light yellow brown surface sediments and dark brown colored subsurface sediments in KODOS-89 area, western part of Clarion-Clipperton fracture zone in north pacific, *J. Oceanol. Soc. Korea.*, **26**: 193-203.

Jung, H.S., K.S. Jeong, K.Y. Lee, J.K. Kang and M.Y. Jung, 1990, Origin of manganese modules and their distribution in the KODOS-89 area, northeastern equatorial Pacific, *J. Oceanol. Soc. Kor.*, **25**: 189-204.

Kadko, D. and L.H. Burckle, 1980, Manganese nodule growth rates determined by fossil diatom dating, *Nature*, **287**: 725-726.

Kang, J.K. and S.J. Han, 1988, Mineralogy, geochemistry and formation of ferromanganese nodules from the KONOD-1 site, northeastern Equatorial Pacific, *J. Oceanol. Soc. Kor.*, **23**: 25-40.

KORDI,1990, A study on the strategy for the development of deep seabed mineral resources (I) (Cruise Report), BSPG 00094-296-5, 1-1093.

KORDI, 1991, A study on the strategy for the development of deep seabed mineral resources (II) (Cruise Report), BSPG 000118-369-5, 1-1093.

KORDI, 1992, A study on the strategy for the development of deep seabed mineral resources (III) (Cruise Report), BSPG 000143-542-5, 1-720

Krishnaswami, S. and J.K. Cochran, 1978, Uranium and thorium series nuclides in oriented ferromanganese nodules: growth rates, turnover times and nuclide behavior, Earth Planet. *Sci. Lett.*, **40**: 45-62.

Krishnaswami, S., J.K. Cochran, K.K. Turekian and M. M. Sarine, 1978, Time scales of deep-sea ferromanganese nodule growth based on Be-10 and alpha track distributions and their relation to uranium series measurements, in: La Genese des Nodules de Manganese, Colloques Internationaux du C.N.R.S., No. 289: 251-260, Gif-sur-Yvette, 25-30 Sept. 1978, Paris, France.

Ku, T.L. and W.S. Broecker, 1969, Radiochemical studies on manganese nodules of deep-sea origin, Deep-Sea Res., **16**: 625-637.

Ku, T.L. and K.G. Knauss, 1979, Radioactive disequilibrium in fissure-filling material and its implication in dating of manganese nodules, in: La Genese des Nodules de Manganese, Colloques Internationaux du C.N.R.S., No. 289: 251-260, Gif-sur-Yvette, 25-30 Sept. 1978, Paris, France.

Ku, T.L., K.G. Knauss and G.G. Mathieu, 1977, Uranium in open ocean: Concentration and isotopic composition, Deep-Sea Research, **24**: 1005-1017.

Ku, T.L., 1976, Rates of manganese accretion. In: Marine Manganese Deposits (ed. G. P. Glasby), Elsevier, Amsterdam, 249-267.

Lyle, M., G. R. Heath and J. M. Robbins, 1984, Transport and release of transition elements during early Diagenesis: sequential leaching of sediments from MANOP Sites M and H. Part 1. pH 5 acetic acid leach. Geochim. Cosmochim. *Acta*, **48**: 1705-1715.

Lynn, D. C. and E. Bonatti, 1965, Mobility of manganese in diagenesis of deep-sea sediments, *Mar. Geol.*, **3**: 457-474.

Moon, D. S., 1993, Uranium-series geochemistry of Pacific ferromanganese nodules and their associated sediments, M. S. thesis, Dept. of Oceanography, Chungnam National University, Taejon. 66p.

Moorby, S. A., D. S. Cronan and G. P. Glasby, 1984, Geochemistry of hydrothermal Mn-oxide deposits from the S. W. pacific island arc. *Geochim. Cosmochim. Acta*, **48**: 433-441.

Moore, W., 1984, Thorium and radium isotopic relationships in manganese nodules and sediments at MANOP Site S, Geochim. Cosmochim. Acta., **48**: 987-992.

Moore, W. S., T. L. Ku , J. D. MacDougall, V. M. Burns, R. Burns, J. Dymond and M. W. Lyle, 1981, Fluxes of metals to a manganese nodule: radiochemical, chemical, structural, and mineralogical studies, Earth Planet. Sci. Lett., **52**: 151-171.

Pettersson, H., 1955, Manganese nodules and oceanic radium, Deep-sea Res., **3**: 335-345.

Piper, D. Z. and B. Fowler, 1980, New constraint on the maintenance of Mn nodules at the sediment surface, *Nature*, **286**: 880-883.

Segl, M., A. Mangini, J. Beer, G. Bonani, M. Suter and W. Wölfli, 1989, Growth rate variations of manganese nodules and crusts induced by paleoceanographic events, *Paleoceanography*, **4**: 511-530.

Sharma, P. and B. L. K. Somayajulu, 1982, Be-10 dating large manganese nodules from world oceans, Earth Planet. Sci. Lett., **59**: 235-244.

Turekian, K. K., J. K. Cochran, W. Krishnaswami, W. A. Lanford, P.D. Parker and K. A. Bouer, 1979, The measurement of Be-10 in manganese nodules using a Tandem Van de Graaff Accelerator, *Geophys. Res. Lett.*, **6**: 417-420.

Von Buttlar, H. and G. Hanterman, 1950, Photographische bestimmung der Aktivitaverteilung in einer Manganknolle der Iiefesee, Naturwissensch aften, **37**: 400-440.

Von Stackelberg, U., 1979, Sedimentation, hiatuses and development of manganese nodules: Valdivia Site VA 13/2, northern central Pacific. In: Marine Geology and Oceanography of the Pacific Manganese Nodule Province, J. L. Bischoff and D. Z. Piper, ed., Plenum, N. Y., 559-586.

Accepted August 8, 1994